



Submerged Sources of Transient Acoustic Emission from Solar Flares

Charles Lindsey¹ , J. C. Buitrago-Casas^{2,3} , Juan Carlos Martínez Oliveros³ , Douglas Braun¹ , Angel D. Martínez⁴ ,
Valeria Quintero Ortega⁴ , Benjamín Calvo-Mozo⁴ , and Alina-Catalina Donea⁵ 

¹North West Research Associates, 3380 Mitchell Lane, Boulder, CO 80301, USA; clindsey@nwra.com

²Physics Department, University of California, Berkeley, CA 94720-7300, USA

³Space Sciences Laboratory, University of California, Berkeley, CA 94720-7450, USA

⁴Observatorio Astronómico Nacional, Universidad Nacional de Colombia, Cra. 30 # 45-03, 111321, Bogotá, Colombia

⁵School of Mathematical Sciences, Monash University, Victoria 3800, Australia

Received 2019 December 16; revised 2020 July 28; accepted 2020 August 6; published 2020 September 21

Abstract

We report the discovery of ultra-impulsive acoustic emission from a solar flare, emission with a seismic signature that indicates submersion of its source approximately a Mm beneath the photosphere of the active region that hosted the flare. Just over two decades ago V. V. Zharkova and A. G. Kosovichev discovered the first acoustic transient released into the Sun's interior by a solar flare. These acoustic waves, refracted back upward to the solar surface after their release, make conspicuous Doppler ripples spreading outward from the flaring region that tell us a lot about their sources. The mechanism by which these transients are driven has stubbornly eluded our understanding. Some of the source regions, for example, are devoid of secondary Doppler, magnetic, or thermal disturbances in the outer atmosphere of the source regions that would signify the driving agent of an intense seismic transient in the outer atmosphere. In this study, we have applied helioseismic holography, a diagnostic based upon standard wave optics, to reconstruct a 3D image of the sources of acoustic waves emanating from the M9.3-class flare of 2011 July 30. These images contain a source component that is submerged a full Mm beneath the active-region photosphere. The signature of acoustic sources this deep in the solar interior opens new considerations into the physics that must be involved in transient acoustic emission from flares—and possibly of flare physics at large. We develop analogies to seismicity remotely triggered by tremors from distant earthquakes, and consider prospects of new insight into the architecture of magnetic flux beneath flaring active regions.

Unified Astronomy Thesaurus concepts: [Solar physics \(1476\)](#); [Helioseismology \(709\)](#); [Solar flares \(1496\)](#)

1. Introduction

We report the discovery of ultra-impulsive acoustic emission from a solar flare, emission whose seismic signature indicates submersion of its source approximately a Mm beneath the photosphere of the active region that hosted the flare. This opens a new promising avenue toward an understanding of the dynamics of transient seismic emission from flares.

A longstanding mystery in local helioseismology has been the occasional emission of *seismic transients* into the solar interior by some solar flares. Discovered by Zharkova & Kosovichev (1998; see also Kosovichev & Zharkova 1998a, 1998b), this emission elicits a clear observational signature at the Sun's surface, as the great preponderance of the energy radiated inward is refracted back to the Sun's surface in the succeeding hour, making conspicuous Doppler ripples that spread several tens of thousands of km outward from the flaring region. Hypotheses proposing mechanisms for this emission have included (1) transient heating of the flaring outer atmosphere (Fisher et al. 1985a, 1985b; Kosovichev & Zharkova 1998a, 1998b; Zharkova & Kosovichev 1998; Donea & Lindsey 2005; Lindsey & Donea 2008; Zharkova 2008; Macrae et al. 2018), such as by energetic electrons accelerated by magnetic fields, and (2) Lorentz-force transients applied directly to the photosphere by flexing magnetic flux (Hudson et al. 2008; Kosovichev 2011; Alvarado-Gómez et al. 2012;

Fisher et al. 2012; Wang & Liu 2010). Observational evidence has encouraged both of these hypotheses in some instances, but inconsistently. Both mechanisms involve the transport of coronal magnetic energy downward through the photosphere and into the solar interior. This makes good sense, as the release of coronal magnetic energy explains many other manifestations of the flare, and the total energy released is hundreds to thousands of times that sufficient to drive the acoustic emission (Lindsey & Donea 2008). However, some flares, e.g., the X2.2-class flare of 2011 February 15 (Kosovichev 2011; Alvarado-Gómez et al. 2012), have shown a conspicuous lack of evidence for either the local heating or magnetic transients required to match the helioseismic sources energetically. Indeed, in this instance, even the local Doppler disturbance in the source region shows little relationship to the source morphology (Alvarado-Gómez et al. 2012), independent of what would drive it. This incongruity has led to speculation among the authors that the basic mechanism that drives the emission is submerged. While the acoustic emission is causally connected to the outer manifestations of the flare, its basic mechanism, perhaps including its free-energy source, is some distance *beneath* the photosphere, hence obscured from direct electromagnetic view.

Most of our own studies have recognized conspicuous transient acoustic emission only out to about 6 mHz, e.g., the flare of 2011 February 15 (Alvarado-Gómez et al. 2012). Limitations imposed by diffraction have somewhat discouraged efforts to discriminate the depths of 6 mHz acoustic sources beneath the solar surface. However, the flare of 2011 February 15 released a strong seismic transient with a spectrum that



Original content from this work may be used under the terms of the [Creative Commons Attribution 4.0 licence](#). Any further distribution of this work must maintain attribution to the author(s) and the title of the work, journal citation and DOI.

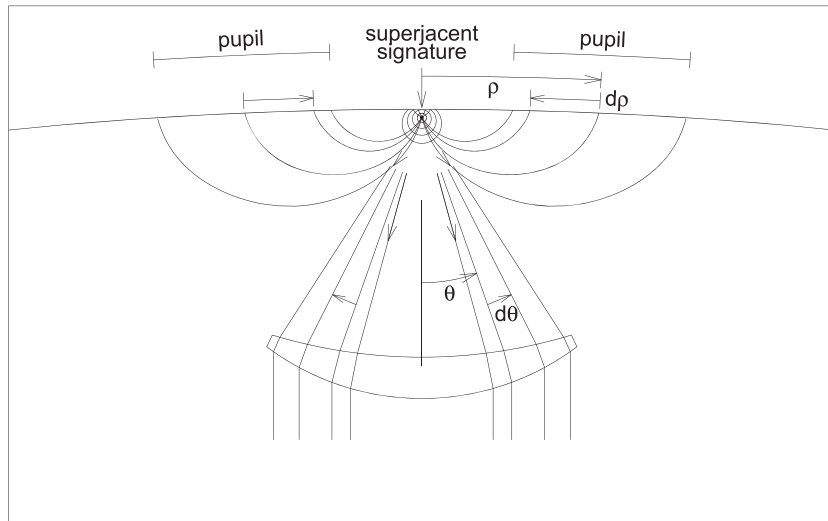


Figure 1. Diagram illustrating parallels between (1) optical imaging by a lens (bottom) of a compact electromagnetic source of waves that travel along straight rays through a uniform medium and (2) computational imaging of an acoustic source of waves propagating along curved rays bent back to the Sun’s surface by refraction. Courtesy of Lindsey & Braun (2000a).

extended out to 10 mHz (Zharkov et al. 2011, 2013). At ~ 670 km, the diffraction limit of 10 mHz emission is considerably finer than of 6 mHz emission, offering depth discrimination approaching scales estimated for magnetic depressions of sunspot umbrae. An extensive survey (Buitrago-Casas et al. 2015) of relatively weak M- and C-class flares has since approximately doubled our database of acoustically active flares in cycle 24. Among these, the M9.3-class flare of 2011 July 30 from AR 11261 (Martínez et al. 2020) released transient emission with multiple distinct 10 mHz source components compact to near the foregoing diffraction limit. (This seismic transient has been independently discovered and studied by Sharykin & Kosovichev 2015.)

2. Procedure

This study is based upon the application of *computational helioseismic holography* (Roddier 1975; Braun et al. 1992, 1998; Lindsey & Braun 1997, 2000a; Lindsey et al. 2011) to 10 mHz helioseismic observations of surface Doppler ripples emanating from the flare of 2011 July 30 in NOAA AR 11261. Helioseismic holography has enjoyed a broad range of applications over the past two decades, from the study of flows in and around active regions (Braun & Lindsey 2000a, 2000b; Braun et al. 2004), monitoring of active regions in the Sun’s far hemisphere (Lindsey & Braun 1990, 2000b, 2017; Braun & Lindsey 2001), modeling the physics of strong absorption of p-modes by magnetic regions (Spruit & Bogdan 1992; Cally 2000, 2007; Schunker et al. 2007, 2008; Lindsey et al. 2007), probing acoustic emission from the solar granulation (Lindsey & Donea 2013), and probing the subphotospheric thermal structures of sunspot umbrae (Lindsey et al. 2010).

Among these has been mapping the source-power density (hereafter “source density”) of acoustic transients emitted by acoustically active flares (Braun et al. 1998; Donea et al. 1999; Donea & Lindsey 2005; Moradi et al. 2007; Lindsey & Donea 2008). Designed along the lines of familiar electromagnetic optics, this diagnostic delivers diffraction-limited acoustic images of the acoustic sources upon which it is focused (Gizon et al. 2018).

Figure 1 illustrates the parallels between optical imaging of a source in the case of (1) the familiar straight-ray geometry of standard electromagnetic optics in a uniform medium at 400–700 THz frequencies and (2) its solar acoustic analog, applied now to 2–10 mHz waves that have been refracted back to the Sun’s surface along curved paths. In the familiar visible optics, the optical element at the bottom of Figure 1 could be the objective lens of a microscope, which beams the waves that encounter it to a charge-coupled device (CCD) far beneath it. The solar acoustic counterpart of the electromagnetic lens captures analogous wave signatures manifested on the Sun’s outlying surface. The essential difference of the latter (solar acoustic) from the former (familiar electromagnetic) is that (1) the optical paths passing through the quiet solar interior *are curved*, due to refraction, and (2) the role of the physical lens in optical reconstruction of an image is taken over by numerical computations.

Figure 2 illustrates the application of helioseismic holography to helioseismic observations of surface Doppler ripples emanating in the (10 ± 1) mHz spectrum from the flare of 2011 July 30. The observations were tracked regional Doppler movies extracted from the database of the Helioseismic and Magnetic Imager (Scherrer et al. 2012) aboard NASA’s space-borne Solar Dynamics Observatory. The middle panel shows a map of the acoustic source density at 02:09:45 TAI, cospatially with the preflare continuum intensity, I_c , (left panel) and the line-of-sight (LOS) magnetic induction, B_{los} (right panel). The source region is a complex δ -configuration sunspot with an eastern umbra of northern-magnetic polarity (bright in panel c) and whose western counterpart is southern-magnetic (dark). The acoustic source density map (middle panel) shows two compact sources conspicuously above the background noise. The source labeled “B,” is planted on the eastern boundary of the eastern umbra. The source labeled “A” is bifurcated, its two kernels, A_{SE} and A_{NW} , straddling a sharp penumbral magnetic precipice (right panel) in which the LOS magnetic field grows from 850 Gauss at the center of kernel A_{NW} to 1150 Gauss at the center of kernel A_{SE} .

Each pixel in the source density map in Figure 3 is the result of a *coherent numerical extrapolation in time reverse* of the myriad acoustic disturbances observed in an annular pupil (see

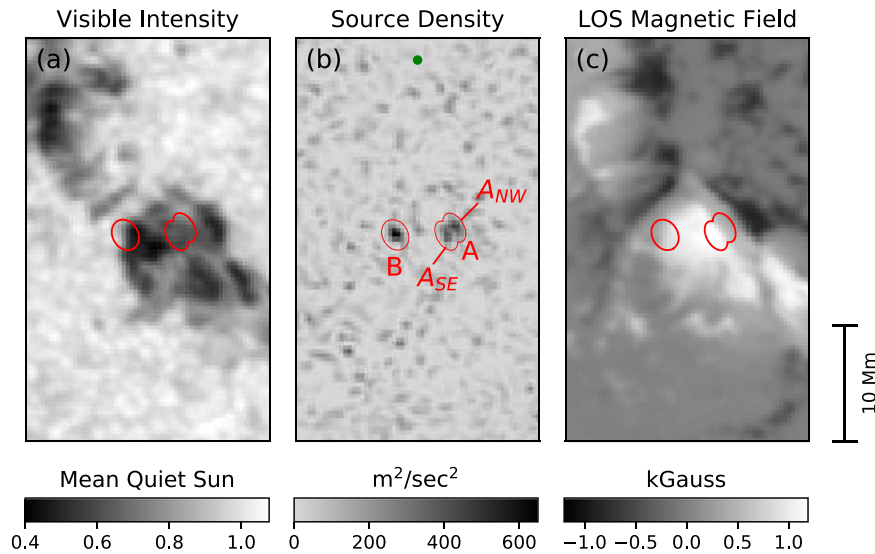


Figure 2. Computational acoustic holography of impulsive acoustic emission emanating from the M9.3-class flare of 2011 July 30 hosted by NOAA AR 11261 during the early impulsive phase of the flare. Panel (b) maps the source density of acoustic radiation released into the 2 mHz spectral band centered at 10 mHz at 02:09:45 TAI. This image is focused at the Sun’s surface. Panels (a) and (c) show cospatial visible-intensity and LOS-magnetic maps, respectively. The filled green circle at top of the middle panel indicates the FWHM of the source density profile of an artificial 10 mHz point source at the base of the photosphere as imaged by the diagnostic that generated the source-density map.

Figure 1) surrounding said pixel downward from the surface along curved optical paths and then back upward to the supposed source at the base of the photosphere, by the rules of wave mechanics in a Standard Solar Model (Christensen-Dalsgaard et al. 1993) devoid of magnetic flux. Computationally, each pixel is treated as the *focal point* of its respective extrapolation. In our applications, the pupil is an annulus with inner radius 7.0 Mm and outer radius 84 Mm centered on the focus. The source density at the focus is equivalent to the square of the amplitude of the wave-mechanical extrapolation at the focus. For a detailed technical elaboration on helioseismic holography as practiced in this study, including Green’s functions that express the foregoing rules of wave mechanics, we refer to Lindsey & Braun (2000a). Further details on our application of helioseismic holography to observations of the flare of 2011 July 30 are elaborated in Martínez et al. (2020).

3. A Depth Diagnostic

Our approach to the question of possible *vertical submersion* of the sources we find now draws upon an optical utility (Braun et al. 1992; Lindsey & Braun 1997, 2000a; Braun et al. 1998) that addresses the question of depth based upon how the *relative focus* of the source density profile varies when the surface back to which the acoustic field is extrapolated is drawn downward, beneath the photosphere.

The top row of Figure 3 shows this diagnostic applied to source A in Figure 2(b), composed of kernels A_{SE} (bottom-left of center, see Figure 2(b) for kernel identifications) and A_{NW} (top-right of center). Starting with the focal plane at the Sun’s surface (top-left panel) and proceeding from left to right, we progressively lower the focal plane—this is the analogy of lowering the microscope at the bottom of Figure 1. As the focal plane submerges, kernel A_{NW} is seen to defocus and fade. At the same time, kernel A_{SE} *contracts into a compact condensation* (red arrow) 840 km beneath the quiet photosphere, becoming the distinctly dominant feature at 1260 km and deeper, ~ 60 km southwest of its original centroid.

Local helioseismology has developed various techniques to model local acoustic anomalies to which it attributes its helioseismic signatures (Skartlien 2001, 2002; Gizon & Birch 2005; Gizon et al. 2009; DeGrave et al. 2018). These might prescribe continuous acoustic source-power distributions in three-dimensions, i.e., source densities with significant extension in both horizontal and vertical directions, to satisfy the helioseismic signatures presented to them. In this study, we go only as far as to show that the signatures imaged in the top row of Figure 3 can be fit definitively by a relatively simple model with acoustic sources that are dipole emitters continuously distributed over a finite set of separate horizontal planes. We prescribe a *forward model* in which the primary emission that contributes to the signature designated A_{NW} in the middle panel of Figure 2 and some of the signature designated A_{SE} is distributed over one relatively shallow horizontal plane, while the primary component that contributes to the signature to which the red arrow points in Figure 3 is distributed in a second plane, one distinctly deeper than the first. The acoustic emission from these source distributions is propagated downward and outward, and eventually back upward, to the overlying surface, prescribed by the same Green’s function that expresses the wave mechanics in the time-reverse extrapolations that lead to the source density maps imaged in the top row of Figure 3. We then apply the same diagnostics to the surface signatures of the disturbances that emanated from the foregoing emitters as we did to the helioseismic observations to get the source density maps imaged in the top row of Figure 3. We then compare the two. The individual depths of the shallow and deep planes in our model are adjusted, along with the source-density distributions in each plane, to minimize the mean square deviation in focal planes at depths 0.2 and 1.1 Mm. To the eventual result we give the name “Model 1,” and this is represented diagrammatically in Figure 4. The acoustic source-density maps that result from Model 1 are imaged in the middle row of Figure 3. The best fit of these maps to those in the top row of Figure 3 was accomplished by fixing the shallow-source plane (magenta) in Model 1 (200 ± 100) km beneath the quiet photosphere, and the deep one (deep blue; 1150 ± 120) km beneath the same.

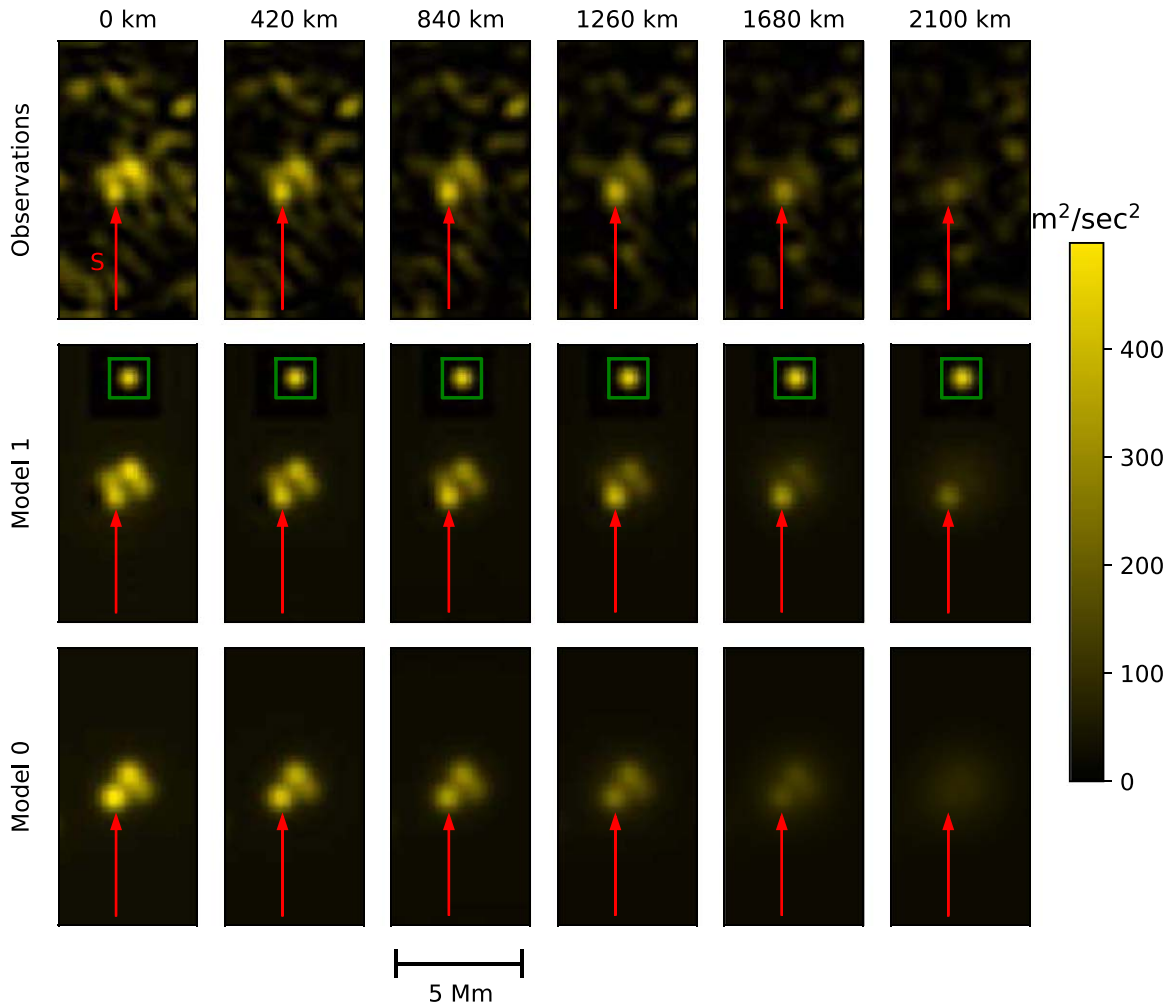


Figure 3. Focus-defocus depth diagnostics of 10 mHz acoustic emission from the flare of 2011 July 30. The top row shows the 10 mHz acoustic source density of source *A* in Figure 2 as the focal plane of the diagnostic is submerged from the base of the quiet solar photosphere to an eventual depth of 2100 km. The red arrow identifies the location of the southwestern end of the southeastern component, A_{SE} , of source *A* in Figure 2. The middle row shows the same acoustic diagnostic applied to the surface disturbance of transients radiated independently by sources prescribed by “Model 1” (see Figure 4) with sources (200 ± 100) and (1150 ± 120) km beneath the quiet photosphere. The compact profile enclosed in a green square at top of each frame in this row shows the signature of an artificial 10 mHz point source in the focal plane of the respective map acoustically radiating into the outlying photosphere. The bottom row shows source densities for a control, “Model 0,” that attempts—unsuccessfully—to reproduce the profiles in the top row with sources confined to a single shallow plane 200 km beneath the photosphere.

Errors attached to the source depths were estimated experimentally, first by studying the statistical character of the egression power of the quiet Sun, avoiding conspicuous acoustic 10 mHz sources. We devised an algorithm based upon this that produces artificial noise that matches the foregoing character, which we then applied to the egression-power signatures mapped in the top row of Figure 3. We reran the modeling procedure on a statistical ensemble of these noisy egression-power signatures, recording the source depths that best fit each of the noise-contaminated egression-power signatures. The errors that we derive, then, are appropriate adjustments of the one-sigma variations in the foregoing respective source depths from their respective means.

For a control of Model 1, we now force the deep source plane upward, to the same depth, 200 km, as the shallow plane, and repeat the best-fit exercise under this constraint. We name the best fit that can be accomplished within this alternative constraint “Model 0.” The source density maps that result from Model 0 are those imaged in the bottom row of Figure 3. This fit, particularly in the 1260 km focal plane or deeper, is

securely unsatisfactory for a match to the helioseismic signatures imaged in the top row.

Model 1, then, prescribes a planar distribution of dipolar emitters at a depth in the range (1150 ± 120) km for the deep signature indicated by the red arrow in Figure 3 and a similarly planar distribution of dipolar emitters for the remainder of the signature at a depth in the range (200 ± 100) km. Sources with some degree of vertical extension above or below the respective source planes may be more realistic for reasons having to do with the physics thought to operate in 3D active-region subphotospheres. This degree of sophistication is left beyond the scope of this study, whose essential finding, then, is a strong indication of a component of flare-triggered transient seismic emission that is of the order of about a Mm beneath the Sun’s surface.

4. Discussion

4.1. Relation of Focus-defocus Depth Diagnostics to Parallax

The focus-defocus depth diagnostic exercised in Figure 3 is closely related to the more familiar one that uses *geometrical*

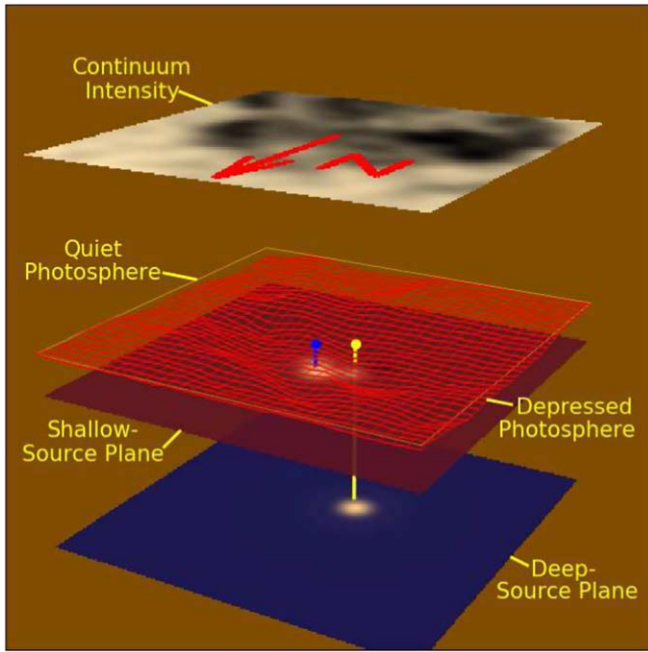


Figure 4. Projection-rendering of “Model 1” that best fits the 10 mHz acoustic source densities mapped in the top row of Figure 3 by distributions of dipole emission over planes 200 (magenta) and 1150 (deep blue) km beneath the quiet photosphere. Each horizontal square panel, obliquely projected to the viewer, is 11.13 Mm across. Vertical displacements are stretched by a factor of five with respect to the horizontal scale. The northwestern “Shallow Source” is marked by a blue peg tacked into the plane 200 km beneath the quiet photosphere. The “Deep Source” is marked by a yellow peg extending just short of the deeper plane 1150 km beneath the quiet photosphere.

parallax to gauge remote distances based upon relative *apparent lateral displacements* of the same subject from separate vantage points. Parallax is useful when the angles subtended by the different vantages of the observations far exceed those of the opening angles of the optics applied to the individual observations. Depth diagnostics based on focus-defocus are useful for a subject with a distance that is relatively nearby compared to the diameter of the objective lens of the instrument viewing it. When viewed by optics with relatively small apertures but from two or more well-separated vantages, differences in relative depth are signified by relative *apparent lateral motion*, a utility upon which our eyes (and stereo microscopes) capitalize. When the opening angle (see θ in Figure 1) becomes large, relative motion of subjects displaced from the focal plane translates to lateral *smearing*, i.e., *defocusing*.

4.2. Magnetic Depression of the Source Domain

Of some interest is that even the shallow source in Model 1 appears to be beneath the quiet photosphere. The question now looms: how does this much shallower submersion compare to a magnetic depression possibly to be expected of the penumbral photosphere? We do not presently have the observational capability to realistically fix the actual depression. This is complicated by the difficult question of how the opacity of a cool magnetic medium could be less than its counterpart in the quiet Sun (Löptien et al. 2018), hence depressing the *optical* surface even if the gas isobar, for example, is not depressed at all. For this study we focus on the magnetic depression (if any) of just the *gas isobar* that marks the base of the quiet photosphere, at a pressure $p_0 = 7.6 \times 10^4$ dyne cm^{-2} in the

Standard Solar Model (Christensen-Dalsgaard et al. 1993). For a rough estimate of this, we propose a physical model in which the sum of the gas pressure,

$$p_g(\text{obs}) = p_0, \quad (1)$$

at the base of the active-region photosphere, and the local magnetic pressure,

$$p_m(\text{obs}) = \frac{B^2(\text{obs})}{8\pi}, \quad (2)$$

is horizontally invariant. This translates to the condition

$$p_{\text{SM}}(z) = p_0 + p_m(\text{obs}), \quad (3)$$

at the depth z to which the magnetic photosphere is depressed, where $p_{\text{SM}}(z)$ signifies the gas pressure of the nonmagnetic Standard Solar Model at depth z . For a model of B^2 to be applied to Equation (2), we solve the Neumann problem to extrapolate a full vector magnetic field, \mathbf{B} , from the observed LOS component (Figure 2(c)). Equations (2) and (3) then deliver the photospheric profile represented by the lattice plotted in red in Figure 4. This depression is 100 km at the horizontal location of kernel A_{NW} and 120 km at the location of kernel A_{SE} . The shallow source in Model 1, then, appears to be about 100 km beneath the magnetically depressed photosphere we model to be directly above it, a margin comparable to the statistical uncertainty in the shallow-source depth.

4.3. Optical Displacement of Virtual Images

The signature of a coherent compact acoustic source deep beneath a flaring photosphere could be a manifestation of various contrivances familiar to standard electromagnetic optics in which the virtual image of a real source is displaced from the actuality. In principle, this leaves significant elements of the two popular hypotheses summarized in the *Introduction* (Hudson et al. 2008; Macrae et al. 2018) possibly eligible for consideration in a new hypothesis as to how acoustic transients might appear to emanate from a source with the apparent depth found by our study. The model of Macrae et al. (2018) features disturbances caused by heating of the outer atmospheres of active regions that penetrate to 4 Mm beneath the quiet photosphere as hypersonic shocks. These shocks are deflected by refractive warpage from the trajectories assumed by helioseismic holography, resulting in a classical caustic when the disturbance is extrapolated back in time reverse assuming no warpage.

4.4. Remotely Triggered Transient Seismic Emission

On the other hand, an acoustic signature vividly consistent with a subsonic, but deeply submerged, highly compact acoustic component is at least strongly suggestive of an actual concentration at some moment of real, localized free energy in the general neighborhood endowed with some measure of transient acoustic potentiality. One phenomenon to consider when the compact localization of a seismic source is highly distinctive from the morphology of overlying disturbances directly visible in electromagnetic radiation has a strong analogy to one in geoseismology: *remote triggering of seismicity* (Hill et al. 1993) by tremors arriving from earthquakes that can be hundreds of km from the sites from which the secondary seismicity emanates. The hypothesis is

that the morphology of the source signature is indicative not only of the tight local compaction of the energy in the acoustic disturbance in the source region immediately following its release, but likewise of the original supply of free energy that fed it. The proposition now is *not* that the release of transient emission is independent of the overlying flare. The temporal relationship between the two secures a concrete causal relationship. It is rather that the part of the flare-induced disturbance that penetrates into the subphotosphere from above acts as a *trigger* releasing confined free energy that has been locally incumbent in magnetohydrodynamic (MHD) conditions in the active-region subphotosphere for some time before the flare began.

Martínez et al. (2020) report that the acoustic transient from kernel A_{SE} in Figure 2 temporally succeeds that from kernel A_{NW} by ~ 200 s. This suggests that the release of different components of the transient at different depths is accomplished by a *trigger* that propagates from the surface downward at a characteristic speed, v_{trig} , of around $(1150 - 200)$ km/200 s = 4.75 km s $^{-1}$. This is about half of the mean sound speed, c , in the Standard Model (Christensen-Dalsgaard et al. 1993), ~ 10.7 km s $^{-1}$, over the 200–1150 km depth range. The Alfvén speed,

$$v_A \equiv \frac{B}{\sqrt{4\pi\rho}}, \quad (4)$$

for a 1150 Gauss magnetic field is less at densities tabulated by the Standard Model more than 200 km beneath the photosphere, beginning at ~ 760 km s $^{-1}$ at that depth. For a magnetic field that maintains this flux density as depth increases, though, the Alfvén speed decreases rapidly, for a cumulative Alfvén travel time of 230 s to the depth of 1150 km. The Alfvén speed can be maintained to 4.75 km s $^{-1}$ by a model that *progressively squeezes* the magnetic flux in which the transient acoustic source is embedded with increasing depth, from as shallow a margin as possible beneath the active-region photosphere overlying the submerged transient acoustic source. This prescribes a flux density of approximately 3000 Gauss at the 1150 km depth.

4.5. Possible Energy Sources

What dynamics might be involved in a hypothesis that proposes a submerged source of free energy to drive transient acoustic emission? Two prospective resources are as follows.

4.5.1. Convective Instability

Up to a few hundred km beneath the photosphere, convective transport of heat is generally understood to be considerably suppressed beneath sunspot umbrae and penumbrae. Cooling of the umbral and penumbral photospheres leads to a superadiabatic temperature gradient that is fundamentally unstable—except that the sudden release of the gravitational energy thus accumulated is resisted by the same magnetic field that suppresses convection in general in sunspots. Could some part this supercooled gas, if slightly jiggled, escape its magnetic constraints to release a conspicuous acoustic transient? Bear in mind that a much weaker superadiabatic thermal gradient than that beneath the sunspot environment is understood to drive p-modes beneath a nonmagnetic photosphere with acoustic

intensities that are a considerable fraction of that released by acoustically active flares.

4.5.2. Magnetic Free Energy

In fairness to Hudson et al. (2008) and Fisher et al. (2012), the prevalence of strong magnetic flux in the general neighborhoods of all known acoustic transients continues to suggest a strong likelihood of the involvement, in some capacity, of Lorentz forces in acoustic-transient emission. Given the strong evidence that said magnetic flux extends deep beneath the photosphere, this would likely apply to a source that is actually submerged. Moreover, it is hard to see how the superadiabatic thermal gradient considered directly above could realistically be made to extend to a depth approaching 1150 km. We understand that free energy in coronal magnetic fields drives flares, and that the total energy released by a flare is generally hundreds to thousands of times that released into the attendant acoustic transient—when there is one. Is it not in fact likely that the magnetic flux that eventually breaks into the Sun’s corona is already highly charged with free energy long before it arrives at the surface? If so, one might propose that the part of the magnetic flux that remains submerged at any moment retains sufficient locally available free energy to drive an acoustic transient—if triggered.

There are broad arguments (Spruit & Bogdan 1992; Cally 2000, 2007; Lindsey et al. 2007; Schunker et al. 2007, 2008) that the coupling of magnetic to compressional energy (hence transfer of free energy from magnetic to acoustic) is most favorable when the magnetic pressure, p_m , is roughly comparable to the gas pressure, p_g . This condition would be consistent with the increase in the magnetic field strength needed to maintain an Alfvén speed of 4.75 km s $^{-1}$ to match the time delay between shallow kernel A_{NW} and deep kernel A_{SE} . If flare acoustic transients *are* driven by submerged magnetic free energy, then what can this tell us about subphotospheric magnetic architecture?

5. Summary

1. The recognition of instances of ultra-impulsive transient acoustic emission from flares has led to unprecedented spatial discrimination of the apparent sources thereof.
2. This has led to recognition of a component of transient acoustic emission with an apparent source that is submerged approximately 1 Mm beneath the active-region photosphere.
3. The evident submergence of transient acoustic sources opens new possibilities as to the mechanics involved in transient acoustic emission from flares. In fact, it offers new, direct insight into the longstanding mystery of transient acoustic sources that show a conspicuous lack of horizontally cospatial disturbances in the outer atmospheres of the active regions that host them.

With the many powerful resources that we now have, especially NASA’s Solar Dynamics Observatory and NSF’s new Daniel K. Inouye Solar Telescope, we look forward to the promise of a very fruitful interdisciplinary new advent in flare seismology approaching the coming solar activity cycle.

We greatly appreciate the insights of Drs. Matthias Rempel and Anna Malanuschenko, and the technical assistance of Dr. Joseph Werne. We also appreciate a very knowledgeable,

conscientious, and thoughtful review by an anonymous referee. The authors are grateful for the support of NASA Grants NNX16AG89G and 80NSSC20K0712.

ORCID iDs

Charles Lindsey  <https://orcid.org/0000-0002-5658-5541>
 J. C. Buitrago-Casas  <https://orcid.org/0000-0002-8203-4794>
 Juan Carlos Martínez Oliveros  <https://orcid.org/0000-0002-2587-1342>
 Douglas Braun  <https://orcid.org/0000-0001-6840-2717>
 Angel D. Martínez  <https://orcid.org/0000-0002-3435-4881>
 Valeria Quintero Ortega  <https://orcid.org/0000-0002-5911-6783>
 Benjamín Calvo-Mozo  <https://orcid.org/0000-0002-5041-1743>
 Alina-Catalina Donea  <https://orcid.org/0000-0002-4111-3496>

References

- Alvarado-Gómez, J. D., Buitrago-Casas, J. C., Martínez-Oliveros, J. C., et al. 2012, *SoPh*, **280**, 335
- Braun, D. C., Birch, A. C., & Lindsey, C. 2004, in ESA Special Publication 559, SOHO 14 Helio- and Asteroseismology: Toward a Golden Future, ed. D. Danesy (Noordwijk: ESA), 337
- Braun, D. C., & Lindsey, C. 2000a, *SoPh*, **192**, 285
- Braun, D. C., & Lindsey, C. 2000b, *SoPh*, **192**, 307
- Braun, D. C., & Lindsey, C. 2001, *ApJL*, **560**, L189
- Braun, D. C., Lindsey, C., Fan, Y., & Fagan, M. 1998, *ApJ*, **502**, 968
- Braun, D. C., Lindsey, C., Fan, Y., & Jefferies, S. M. 1992, *ApJ*, **392**, 739
- Buitrago-Casas, J. C., Martínez Oliveros, J. C., Lindsey, C., et al. 2015, *SoPh*, **290**, 3151
- Cally, P. S. 2000, *SoPh*, **192**, 395
- Cally, P. S. 2007, *AN*, **328**, 286
- Christensen-Dalsgaard, J., Proffitt, C. R., & Thompson, M. J. 1993, *ApJL*, **403**, L75
- DeGrave, K., Braun, D. C., Birch, A. C., Crouch, A. D., & Javornik, B. 2018, *ApJ*, **863**, 34
- Donea, A. C., Braun, D. C., & Lindsey, C. 1999, *ApJL*, **513**, L143
- Donea, A. C., & Lindsey, C. 2005, *ApJ*, **630**, 1168
- Fisher, G. H., Bercik, D. J., Welsch, B. T., & Hudson, H. S. 2012, *SoPh*, **277**, 59
- Fisher, G. H., Canfield, R. C., & McClymont, A. N. 1985a, *ApJ*, **289**, 425
- Fisher, G. H., Canfield, R. C., & McClymont, A. N. 1985b, *ApJ*, **289**, 434
- Gizon, L., & Birch, A. C. 2005, *LRSP*, **2**, 6
- Gizon, L., Fournier, D., Yang, D., Birch, A. C., & Barucq, H. 2018, *A&A*, **620**, A136
- Gizon, L., Schunker, H., Baldner, C. S., et al. 2009, *SSRv*, **144**, 249
- Hill, D. P., Reasenber, P. A., Arabaz, M. W. J., et al. 1993, *Sci*, **260**, 1617
- Hudson, H. S., Fisher, G. H., & Welsch, B. T. 2008, in ASP Conf. Ser. 383, Flare Energy and Magnetic Field Variations, ed. R. Howe et al. (San Francisco, CA: ASP), 221
- Kosovichev, A. G. 2011, *ApJL*, **734**, L15
- Kosovichev, A. G., & Zharkova, V. V. 1998a, in IAU Symp. 185, New Eyes to See Inside the Sun and Stars, ed. F.-L. Deubner, J. Christensen-Dalsgaard, & D. Kurtz (Cambridge: Cambridge Univ. Press), 191
- Kosovichev, A. G., & Zharkova, V. V. 1998b, *Natur*, **393**, 317
- Lindsey, C., & Braun, D. 2017, *SpWea*, **15**, 761
- Lindsey, C., Braun, D., Hernández, I. G., & Donea, A. 2011, in Holography, ed. F. A. M. Ramirez (Rijeka: IntechOpen), 81, <https://www.intechopen.com/books/holography-different-fields-of-application/computational-seismic-holography-of-acoustic-waves-in-the-solar-interior>
- Lindsey, C., & Braun, D. C. 1990, *SoPh*, **126**, 101
- Lindsey, C., & Braun, D. C. 1997, *ApJ*, **485**, 895
- Lindsey, C., & Braun, D. C. 2000a, *SoPh*, **192**, 261
- Lindsey, C., & Braun, D. C. 2000b, *Sci*, **287**, 1799
- Lindsey, C., Cally, P. S., & Rempel, M. 2010, *ApJ*, **719**, 1144
- Lindsey, C., & Donea, A. C. 2008, *SoPh*, **251**, 627
- Lindsey, C., & Donea, A.-C. 2013, *JPhCS*, **440**, 012044
- Lindsey, C., Schunker, H., & Cally, P. S. 2007, *AN*, **328**, 298
- Löptien, B., Lagg, A., van Noort, M., & Solanki, S. K. 2018, *A&A*, **619**, A42
- Macrae, C., Zharkov, S., Zharkova, V., et al. 2018, *A&A*, **619**, A65
- Martínez, A. D., Ortega, V. Q., Buitrago-Casas, J. C., et al. 2020, *ApJL*, **895**, L19
- Moradi, H., Donea, A. C., Lindsey, C., Besliu-Ionescu, D., & Cally, P. S. 2007, *MNRAS*, **374**, 1155
- Rodder, F. 1975, CRASB, **204**, 93
- Scherrer, P. H., Schou, J., Bush, R. I., et al. 2012, *SoPh*, **275**, 207
- Schunker, H., Braun, D. C., & Cally, P. S. 2007, *AN*, **328**, 292
- Schunker, H., Braun, D. C., Lindsey, C., & Cally, P. S. 2008, *SoPh*, **251**, 341
- Sharykin, I. N., & Kosovichev, A. G. 2015, *ApJ*, **808**, 72
- Skartlien, R. 2001, *ApJ*, **554**, 488
- Skartlien, R. 2002, *ApJ*, **565**, 1348
- Spruit, H. C., & Bogdan, T. J. 1992, *ApJL*, **391**, L109
- Wang, H., & Liu, C. 2010, *ApJL*, **716**, L195
- Zharkov, S., Green, L. M., Matthews, S. A., & Zharkova, V. V. 2011, *ApJL*, **741**, L35
- Zharkov, S., Green, L. M., Matthews, S. A., & Zharkova, V. V. 2013, *SoPh*, **284**, 315
- Zharkova, V. V. 2008, *SoPh*, **251**, 665
- Zharkova, V. V., & Kosovichev, A. G. 1998, in ESA Special Publication 418, Structure and Dynamics of the Interior of the Sun and Sun-like Stars, ed. S. Korzenik (Noordwijk: ESA), 661